Adaptive Angle-Constrained Enclosing Control for Multirobot Systems Using Bearing Measurements

Ke Lu, Shi-Lu Dai, Member, IEEE, and Xu Jin, Member, IEEE

Abstract—This paper proposes a constrained control framework to solve the moving-target enclosing problem for non-holonomic multirobot systems, where the safety and precision constraints are considered during the encircling motion. Based on bearing measurements, the target-robot and inter-robot angles are constrained to satisfy the requirements of limited sensing range and collision avoidance. The precision constraint further guarantees all robots converging to a small neighbourhood of the desired enclosing formation. With the help of adaptive estimators, universal barrier Lyapunov functions are employed to the constrained control framework despite the lack of target's velocity. Simulation results verify the effectiveness of the proposed control algorithm.

Index Terms—Enclosing control, angle constraints, collision avoidance, nonholonomic mobile robots, limited sensing range.

I. INTRODUCTION

Coordination and control of multiagent systems have received great attention in many fields [1]-[4] due to promising applications such as surveillance, search, rescue, etc. Target enclosing control is an important problem in multiagent coordination, where an enclosing formation is utilized to entrap, attack, protect, and monitor a target. A great number of control design techniques have been presented for the target enclosing problem [5]-[18], where mobile agents are driven to enclose a static or moving target. In enclosing control tasks, many works generate a desired formation based on relative distances or positions. Compared with position or distance sensors, bearing-only sensors are simpler and cheaper, which promotes the advance in bearing-based formation control [19]–[21]. Consequently, control designs based on bearing measurements have been developed in the target enclosing control literature [10]–[12], in which a fixed or time-varying formation is achieved around the target. However, most of the

The work of Ke Lu and Shi-Lu Dai was supported in part by the National Natural Science Foundation of China under Grant 61973129, Grant 42227901, Grant 62273156, and Grant 62073090, in part by the Guangdong Basic and Applied Basic Research Foundation under Grant 2021A1515012004, and in part by the Innovation Group Project of Southern Marine Science and Engineering Guangdong Laboratory (Zhuhai) (No. SML2022008). The work of Xu Jin was supported in part by the United States National Science Foundation under Grant 2131802. (Corresponding author: Shi-Lu Dai.)

Ke Lu is with the School of Automation Science and Engineering, South China University of Technology, Guangzhou 510641, China (e-mail: lukenan-lin@163.com).

Shi-Lu Dai is with the School of Automation Science and Engineering, Key Laboratory of Autonomous Systems and Networked Control of Ministry of Education, South China University of Technology, Guangzhou 510641, China, and also with the Southern Marine Science and Engineering Guangdong Laboratory (Zhuhai), Zhuhai 519000, China (e-mail: audaisl@scut.edu.cn).

Xu Jin is with the Department of Mechanical and Aerospace Engineering, University of Kentucky, Lexington, KY 40506 USA (e-mail: xu.jin@uky.edu).

existing target enclosing control algorithms do not consider any constraint requirement.

In enclosing control tasks, safety is typically a primary concern, which requires that autonomous agents cannot go beyond some predefined ranges. In practice, an onboard sensor only can work effectively within a certain range due to the limited sensing capability [22]-[24]. In addition, as a practical problem, collision avoidance with the target or neighbouring agents has been addressed in the enclosing control literature [11]-[18]. In [11], a maximum allowed subtended angle is employed to guarantee collision avoidance with a disk target. Furthermore, a precise formation for multiagent systems usually requires small formation tracking errors during the transient and steady-state stages [25], [26]. The precision constraint has been addressed in synchronization control [27], formation maneuvering [28], and path-following control [29]. How to develop a constrained control framework for the target enclosing problem, such that both safety and formation precision are addressed, is a challenging research topic that has not been fully considered in the enclosing control literature.

The constrained control design can prevent multiagent systems violating some certain limits specified by different constraint requirements such as safety and line-of-sight range [30]–[33]. Barrier Lyapunov functions (BLFs) are usually incorporated with control design to deal with the constrained systems [34]–[36]. In [34], an asymmetric BLF is employed to handle output-constrained nonlinear systems. Both symmetric and asymmetric BLFs are applied to prevent the violation of full state constraints [35]. A novel universal BLF proposed in [36] can not only address asymmetric and symmetric constraint requirements, but also work for the system with no constraints. Therefore, how to extend the BLF-based controller design to constrained enclosing control systems is another motivation for this work.

In this work, we develop a constrained control framework to solve the moving-target enclosing problem for nonholonomic multirobot systems with safety and precision requirements. Based on bearing measurements, the target-robot and interrobot angles are constrained to guarantee the limited sensing range and collision avoidance with the target and neighbouring robots. Universal BLFs and adaptive estimators are incorporated with bearing-angle-based control strategy to satisfy all constraint requirements despite the lack of target's velocity. The contributions of this work are summarized as follows.

- (i) A constrained control framework is proposed to solve the moving-target enclosing problem with the concern of both safety and precision constraints.
- (ii) The angle constraints related to the safety are addressed, which enables mobile robots to avoid collisions with the

target and neighbouring robots while guaranteeing the limited sensing requirement.

(iii) The precision constraint, which requires small formation tracking errors, enforces mobile robots to converge to a desired enclosing formation despite the lack of accurate knowledge of target's velocity.

II. PROBLEM FORMULATION

Consider a moving target is enclosed by a team of $n \geq 2$ nonholonomic mobile robots in a plane. For convenience of presentation, we define the index set $\mathcal{N} = \{1, ..., n\}$. The kinematics of nonholonomic robot $i, i \in \mathcal{N}$, is modeled as

$$\dot{p}_i(t) = \begin{bmatrix} \cos \theta_i(t) \\ \sin \theta_i(t) \end{bmatrix} v_i(t)$$

$$\dot{\theta}_i(t) = \omega_i(t)$$
(1)

where $p_i(t) = [x_i(t) \ y_i(t)]^T \in \mathbb{R}^2$ is the robot's position with respect to the global coordinate frame, $\theta_i(t)$ is the heading angle of the ith robot, and $v_i(t)$ and $\omega_i(t)$ are the linear and angular velocity control inputs, respectively. As shown in Fig. 1, an onboard sensor is installed at the position $p_{si}(t) = [x_{si}(t) \ y_{si}(t)]^T \in \mathbb{R}^2$, which is shifted a non-zero distance d from $p_i(t)$ along direction $\theta_i(t)$. The position $p_{si}(t)$ is described by $p_{si}(t) = p_i(t) + d[\cos\theta_i(t) \sin\theta_i(t)]^T$, whose dynamics is modeled as

$$\dot{p}_{si}(t) = G_i(t)u_i(t) \tag{2}$$

with $u_i(t) = [v_i(t) \ \omega_i(t)]^T$, where $G_i(t)$ is defined as

$$G_i(t) = \begin{bmatrix} \cos \theta_i(t) & -d \sin \theta_i(t) \\ \sin \theta_i(t) & d \cos \theta_i(t) \end{bmatrix}.$$
 (3)

Note that $\det(G_i(t)) = d$, which implies that $G_i(t)$ is *invertible* if $d \neq 0$. The moving target is governed by $\dot{p}_0(t) = v_0(t)$, where $p_0(t) = [x_0(t) \ y_0(t)]^T \in \mathbb{R}^2$ and $v_0(t) \in \mathbb{R}^2$ are the position and velocity of the target, respectively. The relative distance between the onboard sensor and the moving target is defined as $\rho_i(t) = \sqrt{(x_0(t) - x_{si}(t))^2 + (y_0(t) - y_{si}(t))^2}$ whose derivative yields

$$\dot{\rho}_i(t) = -\varphi_i^T(t)[\dot{p}_{si}(t) - v_0(t)] \tag{4}$$

with $\varphi_i(t) = [p_0(t) - p_{si}(t)]/\rho_i(t) = [\cos \phi_i(t) \sin \phi_i(t)]^T$, where $\varphi_i(t)$ is the measurable unit vector from the onboard sensor pointing to the target, and $\phi_i(t)$ is the bearing angle to the target with respect to the onboard sensor as shown in Fig. 1. The unit vector $\bar{\varphi}_i(t)$ is orthogonal to $\varphi_i(t)$, which is described as $\bar{\varphi}_i(t) = [\cos(\phi_i(t) \pm \frac{\pi}{2}) \sin(\phi_i(t) \pm \frac{\pi}{2})]^T$ where $\pm \frac{\pi}{2}$ denotes the opposite directions being orthogonal to $\varphi_i(t)$.

A. Target-Robot Angle Constraint

It is assumed that the onboard sensor only provides bearing measurements, rather than distance information, e.g., $\rho_i(t)$ defined in (4). Specifically, as shown in Fig. 1, two points p_{TLi} and p_{TRi} on the surface of a disk target can be detected via an onboard sensor, e.g., a monocular cameral system, and thus the bearing measurements g_{TLi} , g_{TRi} , and φ_i are obtained, where

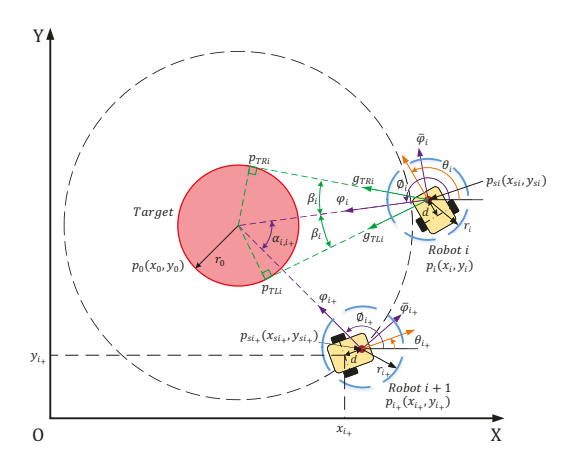


Fig. 1. Illustration of enclosing a disk target by multiple mobile robots.

the subtended angle $\beta_i(t) \in (0, \pi/2)$ is further available. According to geometrical relation shown in Fig. 1, we have

$$\rho_i(t) = \frac{r_0}{\sin \beta_i(t)} \tag{5}$$

where r_0 denotes the radius of the target. The derivative of (5) along system (4) produces

$$\dot{\beta}_i(t) = \varphi_i^T(t) \frac{\sin^2 \beta_i(t)}{r_0 \cos \beta_i(t)} [\dot{p}_{si}(t) - v_0(t)]. \tag{6}$$

Note that $\sin\beta_i(t)\in(0,1)$ is strictly monotonically increasing with $\beta_i(t)\in(0,\pi/2)$, and it is clear from (5) that $\rho_i(t)$ has the maximal value as $\beta_i(t)\to\beta_{\min,i}$ and has the minimal value as $\beta_i(t)\to\beta_{\max,i}$, where $\beta_{\min,i}$ and $\beta_{\max,i}$ are the minimal and maximal subtended angles, respectively. Hence, the target-robot angle constraint

$$\beta_{\min,i} < \beta_i(t) < \beta_{\max,i} \tag{7}$$

ensures the limited sensing range and collision avoidance with a target. In terms of the geometrical relation, the selection of $\beta_{\min,i}$ and $\beta_{\max,i}$ should satisfy $\underline{\rho}_i \leq \frac{r_0}{\sin\beta_{\max,i}} < \rho_i(t) < \frac{r_0}{\sin\beta_{\min,i}} \leq \bar{\rho}_i$, where $\underline{\rho}_i \geq r_i + r_0$ and $\bar{\rho}_i$ denote the minimal and maximal relative distances, respectively, and r_i is the safety radius of the robot i. However, the target's radius r_0 is not necessarily needed for converting $\underline{\rho}_i$ and $\bar{\rho}_i$ to $\beta_{\min,i}$ and $\beta_{\max,i}$. For example, by setting the robot close enough to a disk target, the measured subtended angle can be specified as $\beta_{\max,i}$. This corresponds to the constraints $\underline{\rho}_i$ and $\bar{\rho}_i$ required to be known a prior in the distance-based framework. Define the subtended angle error as

$$e_{\beta i}(t) = \beta_i(t) - \beta_{\text{des},i} \tag{8}$$

where $\beta_{\text{des},i}$ is the desired subtended angle with $\beta_{\min,i} < \beta_{\text{des},i} < \beta_{\max,i}$. Substituting (8) into (7) yields

$$-\underline{e}_{\beta i} < e_{\beta i}(t) < \bar{e}_{\beta i} \tag{9}$$

where $\underline{e}_{\beta i} = \beta_{\text{des},i} - \beta_{\min,i}$ and $\bar{e}_{\beta i} = \beta_{\max,i} - \beta_{\text{des},i}$.

Remark 1: Instead of a fixed camera, a monocular camera is mounted on a pan-tilt unit at position p_{si} such that it can rotate about the axis perpendicular to the moving plane of the robot. The subtended angle β_i is invariant represented in different coordinates, e.g., camera and robot coordinates, and

thus it can be directly applied to the controllers. With the concern of the inherent limitation of a camera, the selected $\beta_{\max,i}$ is required to be less than the limited angle of view.

B. Inter-Robot Angle Constraint

The target-robot angle constraint (7) implies the existence of a minimal distance $\underline{\rho}_i$. According to the arc length formula, the existence of a minimal distance between neighbouring robots results from the minimal radius $\underline{\rho}_i$ and the corresponding minimal inter-robot angle, which establishes neighbouring robot collision avoidance. Let the index set $\overline{\mathcal{N}} = \mathcal{N} \setminus n$, and define the driving robot, i.e., robot n, which is assigned with an encircling speed. Then, its pre-neighbor robot n-1 is defined in the clockwise or counterclockwise radial order around the target according to the encircling motion direction. In terms of this definition, the robot $i, i \in \overline{\mathcal{N}}$, has its next-neighbouring robot i+1 labeled as i_+ for convenience of presentation. As shown in Fig. 1, we define the separation angle α_{i,i_+} to describe the inter-robot angle between the robot $i, i \in \overline{\mathcal{N}}$, and its next neighbour i_+ , which can be calculated as

$$\alpha_{i,i_{+}}(t) = \cos^{-1}(\varphi_i^T(t)\varphi_{i_{+}}(t))$$

where $\cos^{-1}(\cdot)$ is the inverse cosine function. The robot i is assumed to have only access to $\varphi_{i_+}(t)$ from its neighbour i_+ via local communication. According to the neighbouring robot definition, the first robot (robot 1) is the next neighbour of the robot n. Define their separation angle as

$$\alpha_{n,1}(t) = 2\pi - \sum_{i \in \bar{\mathcal{N}}} \alpha_{i,i_+}(t) \tag{10}$$

which implies that the separation angle $\alpha_{n,1}(t)$ relates to the rest of separation angles $\alpha_{i,i_+}(t)$. Besides, the lower bound of $\alpha_{n,1}(t)$ relies on the upper bounds of $\alpha_{i,i_+}(t)$, that is, $\underline{\alpha}_{n,1} \leq 2\pi - \sum_{i \in \overline{\mathcal{N}}} \bar{\alpha}_{i,i_+}$, which prevents collision between the first and the last robots. Hence, the inter-robot angle constraint

$$\underline{\alpha}_{i,i_{+}} < \alpha_{i,i_{+}}(t) < \bar{\alpha}_{i,i_{+}}, \ i \in \bar{\mathcal{N}}$$
(11)

ensures collision avoidance between each robot and its next neighbour, where $\underline{\alpha}_{i,i_+}$ and $\bar{\alpha}_{i,i_+}$ are the minimal and maximal separation angles, respectively. The separation angle error is defined as

$$e_{\alpha i}(t) = \alpha_{i,i_+}(t) - \alpha_{\text{des},i,i_+}, \ i \in \bar{\mathcal{N}}$$
 (12)

where $\alpha_{{\rm des},i,i_+}$ is the desired separation angle with $\underline{\alpha}_{i,i_+} < \alpha_{{\rm des},i,i_+} < \bar{\alpha}_{i,i_+}$. Substituting (12) into (11) produces

$$-\underline{e}_{\alpha i} < e_{\alpha i}(t) < \bar{e}_{\alpha i}, \ i \in \bar{\mathcal{N}}$$
 (13)

where $\underline{e}_{\alpha i} = \alpha_{{\rm des},i,i_+} - \underline{\alpha}_{i,i_+}$ and $\bar{e}_{\alpha i} = \bar{\alpha}_{i,i_+} - \alpha_{{\rm des},i,i_+}$.

Remark 2: According to the definition of neighbouring robots, the desired separation angle $\alpha_{\mathrm{des},n,1}$ between the first and the last robots is not specified and it relies on $\alpha_{\mathrm{des},i,i_+}$, that is, $\alpha_{\mathrm{des},n,1}=2\pi-\sum_{i\in\bar{\mathcal{N}}}\alpha_{\mathrm{des},i,i_+}$. The separation angle error $e_{\alpha n}(t)=\alpha_{n,1}(t)-\alpha_{\mathrm{des},n,1}=-\sum_{i\in\bar{\mathcal{N}}}e_{\alpha i}(t)$ in view of (10), which indicates that the separation angle error $e_{\alpha n}(t)$ depends on the sum of separation angle errors between the robot i and its neighbour i_+ . Thus, a small error $e_{\alpha n}(t)$ requires that all errors $e_{\alpha i}(t)$, $i\in\bar{\mathcal{N}}$, converge to small neighborhoods of zero.

C. Precision Constraint

To ensure a precise formation, it requires that the angle error constraints (9) and (13) are further restricted by

$$-\Omega_{\beta i}(t) < e_{\beta i}(t) < \bar{\Omega}_{\beta i}(t) \tag{14}$$

$$-\underline{\Omega}_{\alpha i}(t) < e_{\alpha i}(t) < \bar{\Omega}_{\alpha i}(t) \tag{15}$$

where $\underline{\Omega}_j(t) > 0$ and $\bar{\Omega}_j(t) > 0$, $j = \beta i, \alpha i$, are designed decreasing \mathcal{C}^1 functions such that the angle errors $e_{\beta i}(t)$ and $e_{\alpha i}(t)$ are driven to small neighbourhoods of zero as time evolves. Besides, $\bar{\Omega}_j(t)$ and $\underline{\dot{\Omega}}_j(t)$ require to be bounded which is associated with the boundedness of control signals. Moreover, the constraint requirements (14) and (15) should further satisfy the angle error constraints (9) and (13), respectively, that is, $-\underline{e}_j \leq -\underline{\Omega}_j(t) < e_j(t) < \bar{\Omega}_j(t) \leq \bar{e}_j$, $j = \beta i, \alpha i$.

Remark 3: As discussed in Remark 2, small separation angle errors $e_{\alpha i}$, $i \in \bar{\mathcal{N}}$, are preferred. Thus, the precision constraints are further considered to obtain a precise formation. Accordingly, time-varying precision constraints (14) and (15) are designed to ensure that not only subtended angle errors but also separation angle errors should not deviate much from zero. As a result, the robot group is driven to surround a moving target with a precise enclosing formation, despite the lack of accurate knowledge of target's velocity.

Assumption 1: At the initial time t=0, the robots do not violate the angle constraints (7) and (11), that is, $\beta_{\min,i} < \beta_i(0) < \beta_{\max,i}, \ i \in \mathcal{N}$, and $\underline{\alpha}_{i,i_+} < \alpha_{i,i_+}(0) < \bar{\alpha}_{i,i_+}, \ i \in \bar{\mathcal{N}}$. Assumption 2: The target's velocity is bounded, i.e.,

 $||v_0|| \le \bar{v}_0$, where $\bar{v}_0 > 0$ is a constant. Lemma 1: [37] For any constant $\varepsilon > 0$ and any variable $z \in \mathbb{R}$, we have $0 \le |z| - \frac{z^2}{\sqrt{z^2 + \varepsilon^2}} < \varepsilon$.

III. TARGET ENCLOSING CONTROL OBJECTIVE

Under Assumptions 1–2, the target enclosing control objective is to design the feedback control law $u_i(t)$ such that

- (i) the subtended angle $\beta_i(t)$ and the separation angle $\alpha_{i,i_+}(t)$ eventually converge to a small neighborhood of the desired angles $\beta_{\text{des},i}$ and $\alpha_{\text{des},i,i_+}$, respectively; and
- (ii) every robot can avoid collisions with the target and its next-neighbouring robot, while guaranteeing the limited sensing requirement during the encircling motion.

To deal with the constraint requirements, the following universal barrier function [36] is applied in the control design

$$V_j = \frac{1}{2}\eta_j^2, \ \eta_j = \frac{\bar{\Omega}_j \underline{\Omega}_j e_j}{(\bar{\Omega}_j - e_j)(e_j + \underline{\Omega}_j)}, \ j = \beta i, \alpha i$$
 (16)

where η_j is the transformed error variable, which has the following properties: i) $\eta_j=0$ if and only if $e_j=0$; ii) $\eta_j\to-\infty$ when $e_j\to-\underline{\Omega}_j$; and iii) $\eta_j\to+\infty$ when $e_j\to\bar{\Omega}_j$. The derivative of η_j produces

$$\dot{\eta}_{j} = \frac{\partial \eta_{j}}{\partial \bar{\Omega}_{j}} \dot{\bar{\Omega}}_{j} + \frac{\partial \eta_{j}}{\partial \underline{\Omega}_{i}} \dot{\underline{\Omega}}_{j} + \frac{\partial \eta_{j}}{\partial e_{j}} \dot{e}_{j}, \ j = \beta i, \alpha i$$
 (17)

where

$$\begin{split} \frac{\partial \eta_j}{\partial \bar{\Omega}_j} &= \frac{-\underline{\Omega}_j e_j^2}{(\bar{\Omega}_j - e_j)^2 (e_j + \underline{\Omega}_j)}, \ \frac{\partial \eta_j}{\partial \underline{\Omega}_j} = \frac{\bar{\Omega}_j e_j^2}{(\bar{\Omega}_j - e_j) (e_j + \underline{\Omega}_j)^2} \\ \frac{\partial \eta_j}{\partial e_j} &= \frac{\bar{\Omega}_j \underline{\Omega}_j (\bar{\Omega}_j \underline{\Omega}_j + e_j^2)}{(\bar{\Omega}_j - e_j)^2 (e_j + \underline{\Omega}_j)^2}. \end{split}$$

The control laws for the robot $i, i \in \mathcal{N}$, are taken as

$$u_{i} = G_{i}^{-1} \left(\varphi_{i} u_{1i} + \bar{\varphi}_{i} u_{2i} - \varphi_{i} \hat{u}_{1i} - \bar{\varphi}_{i} \hat{u}_{2i} \right), \ i \in \bar{\mathcal{N}} \quad (18)$$

$$u_{i} = G_{i}^{-1} \left(\varphi_{i} u_{1i} - \varphi_{i} \hat{u}_{1i} + \bar{\varphi}_{i} \frac{\bar{\omega}}{\sin \beta_{i}} \right), \ i = n \quad (19)$$

with

$$\begin{split} u_{1i} &= \frac{\cos\beta_{i}}{\sin^{2}\beta_{i}} \bigg(-k_{1i}\bar{\Omega}_{\beta i}\underline{\Omega}_{\beta i}\eta_{\beta i} - \eta_{\beta i}\frac{\partial e_{\beta i}}{\partial\bar{\Omega}_{\beta i}}\frac{\partial\eta_{\beta i}}{\partial\bar{\Omega}_{\beta i}}\dot{\bar{\Omega}}_{\beta i}^{2} \\ &- \eta_{\beta i}\frac{\partial e_{\beta i}}{\partial\underline{\Omega}_{\beta i}}\frac{\partial\eta_{\beta i}}{\partial\underline{\Omega}_{\beta i}}\dot{\underline{\Omega}}_{\beta i}^{2} \bigg) \\ u_{2i} &= \frac{1}{\sin\beta_{i}} \bigg(-k_{2i}\bar{\Omega}_{\alpha i}\underline{\Omega}_{\alpha i}\eta_{\alpha i} - \eta_{\alpha i}\frac{\partial e_{\alpha i}}{\partial\bar{\Omega}_{\alpha i}}\frac{\partial\eta_{\alpha i}}{\partial\bar{\Omega}_{\alpha i}}\dot{\bar{\Omega}}_{\alpha i}^{2} \\ &- \eta_{\alpha i}\frac{\partial e_{\alpha i}}{\partial\underline{\Omega}_{\alpha i}}\frac{\partial\eta_{\alpha i}}{\partial\underline{\Omega}_{\alpha i}}\dot{\underline{\Omega}}_{\alpha i}^{2} - \eta_{\alpha i}\frac{\partial\eta_{\alpha i}}{\partial e_{\alpha i}} \bigg) \\ \hat{u}_{1i} &= \hat{v}_{i0}\frac{H_{1i}}{\sqrt{H_{1i}^{2} + \varepsilon^{2}}}, \quad \hat{u}_{2i} &= \hat{v}_{i0}\frac{H_{2i}}{\sqrt{H_{2i}^{2} + \varepsilon^{2}}} \\ H_{1i} &= \eta_{\beta i}\frac{\partial\eta_{\beta i}}{\partial e_{\beta i}}\frac{\sin^{2}\beta_{i}}{\cos\beta_{i}}, \quad H_{2i} &= \eta_{\alpha i}\frac{\partial\eta_{\alpha i}}{\partial e_{\alpha i}}\sin\beta_{i} \end{split}$$

where $k_{1i}>0$ and $k_{2i}>0$ are control gains, φ_i and $\bar{\varphi}_i$ are unit vectors defined in (4), G_i^{-1} is the inverse matrix defined in (3), $\varepsilon>0$ and $\bar{\omega}>0$ are design parameters, and \hat{v}_{i0} is the estimate of the upper bound of velocity \bar{v}_0 with the estimation error $\tilde{v}_{i0}=\hat{v}_{i0}-\bar{v}_0$. The adaptive laws \hat{v}_{i0} are designed as

$$\dot{\hat{v}}_{i0} = \gamma_i \left(-\sigma_i \hat{v}_{i0} + \frac{H_{1i}^2}{\sqrt{H_{1i}^2 + \varepsilon^2}} + \frac{H_{2i}^2}{\sqrt{H_{2i}^2 + \varepsilon^2}} \right), \ i \in \bar{\mathcal{N}}$$
(20)

$$\dot{\hat{v}}_{i0} = \gamma_i \left(-\sigma_i \hat{v}_{i0} + \frac{H_{1i}^2}{\sqrt{H_{1i}^2 + \varepsilon^2}} \right), \ i = n$$
 (21)

where $\gamma_i > 0$ and $\sigma_i > 0$ are design parameters. The separation angle describes the difference in bearing angles between neighbouring robots in view of (4), which implies that the dynamics of separation angle reflects the difference in the rate of change of bearing angles, that is,

$$\dot{\alpha}_{i,i_{+}} = \dot{\phi}_{i} - \dot{\phi}_{i_{+}}, \ i \in \bar{\mathcal{N}}$$
 (22)

where for an encircling motion, the dynamics of bearing angle can be obtained as

$$\dot{\phi}_i = \frac{\bar{\varphi}_i^T(\dot{p}_{si} - v_0)}{\rho_i}, \ i \in \mathcal{N}. \tag{23}$$

Remark 4: The controller (19) indicates that the robot n assigned with the encircling speed $\bar{\varphi}_i(t) \frac{\bar{\omega}}{\sin\beta_i(t)}$ is constrained by the moving target only. By contrast, the controller (18) lacks the encircling speed term but has the extra terms about $\eta_{\alpha i}$. This indicates that the robot $i, i \in \bar{\mathcal{N}}$, is constrained by the moving target and its neighbour i_+ in two directions $\varphi_i(t)$ and $\bar{\varphi}_i(t)$, respectively. Consequently, the controller (18) needs to simultaneously handle two constraint requirements.

Remark 5: The encircling speed $\bar{\varphi}_i(t) \frac{\bar{\omega}}{\sin\beta_i(t)}$ can be treated as an external disturbance that forces the whole formation to revolve around a moving target. It follows from (12) and (22) that the convergence of separation angle error $e_{\alpha i}(t)$ results from both dynamics $\dot{\phi}_i$ and $\dot{\phi}_{i_+}$. However, the robot $i, i \in \bar{\mathcal{N}}$,

has only access to bearing information without the knowledge of $\dot{\phi}_{i_+}$ from its neighbour. With the higher magnitude of the encircling speed, the separation angle may not converge to its desired value, which implies an enclosing formation distortion. To deal with such a problem, the precision constraint is introduced to ensure the convergence to a correct formation. As a result, when any robot is assigned with an encircling speed, the rest of robots are driven by their neighbours to revolve around a target with small formation tracking errors.

Remark 6: The control laws (18) and (19) require that $G_i(t)$ defined in (3) is invertible with $d \neq 0$. If such a condition is removed, the velocity control inputs v_i and w_i in (1) need to be further designed under the same constrained control framework, where u_i in (18) and (19) are treated as the desired inputs u_{id} without G_i^{-1} . Specifically, u_{id} has the form $u_{id} = \varphi_i u_{1id} + \bar{\varphi}_i u_{2id}$ which can be written as

$$u_{id} = \begin{bmatrix} u_{idx} \\ u_{idy} \end{bmatrix} = \begin{bmatrix} u_{1id}\cos\phi_i + u_{2id}\sin\phi_i \\ u_{1id}\sin\phi_i - u_{2id}\cos\phi_i \end{bmatrix}$$

and the desired heading angle θ_{id} is defined as $\theta_{id} = \arctan(\frac{u_{idy}}{u_{idx}})$ for $u_{id} \neq 0$, and $\theta_{id} = 0$ for $u_{id} = 0$. The control objective is to drive the robot's heading angle θ_i to align with the desired heading angle θ_{id} , and then the magnitude of v_i is the same as $||u_{id}||$. It follows from (8), (12), and (16)–(21) that the variables in u_{id} are $\bar{\Omega}_{ji}$, $\underline{\Omega}_{ji}$, $\dot{\bar{\Omega}}_{ji}$, $\dot{\bar{\Omega}}_{ji}$, $\dot{\bar{\Omega}}_{i0}$, β_i , α_{i,i_+} , ϕ_i , $j=\beta,\alpha$, which implies that $\dot{u}_{idk}=F_k+\frac{\partial u_{idk}}{\partial \beta_i}\dot{\beta}_i+\frac{\partial u_{idk}}{\partial \alpha_{i,i_+}}\dot{\alpha}_{i,i_+}+\frac{\partial u_{idk}}{\partial \phi_i}\dot{\phi}_i$, k=x,y, where F_k consists of the derivative of u_{idk} with respect to $\bar{\Omega}_{ji}$, $\underline{\Omega}_{ji}$, $\dot{\bar{\Omega}}_{ji}$, and $\dot{\bar{v}}_{i0}$, and thus F_k is known, whereas v_0 , $\dot{\phi}_{i_+}$, r_0 , and ρ_i are unknown in the rest parts of \dot{u}_{idk} . Define the angle error and its derivative as

$$e_{\theta i} = \theta_i - \theta_{id}, \quad \dot{e}_{\theta i} = w_i - \dot{\theta}_{id}.$$

To avoid the singularity issue, the angle error is restricted inside a feasible region, that is, $-\underline{e}_{\theta i} \leq -\underline{\Omega}_{\theta i}(t) < e_{\theta i} < \bar{\Omega}_{\theta i}(t) \leq \bar{e}_{\theta i}$, with $\underline{e}_{\theta i} = \bar{e}_{\theta i} \leq \pi/2$. Then, the control laws are designed as

$$v_i = \frac{1}{\cos e_{\theta i}} ||u_{id}||, \quad w_i = u_{\theta i} + \bar{u}_{\theta i} + \hat{u}_{\theta i}$$

where $u_{\theta i} = -k_{3i}\bar{\Omega}_{\theta i}\underline{\Omega}_{\theta i}\eta_{\theta i} - \frac{\partial e_{\theta i}}{\partial\Omega_{\theta i}}\dot{\Omega}_{\theta i} - \frac{\partial e_{\theta i}}{\partial\Omega_{\theta i}}\dot{\Omega}_{\theta i}$, $\bar{u}_{\theta i} = u_{i_F} + \frac{\tan e_{\theta i}}{\eta_{\theta i}}\frac{\partial e_{\theta i}}{\partial\eta_{\theta i}}[H_{2i}(u_{1i}-\hat{u}_{1i})-H_{1i}(u_{2i}-\hat{u}_{2i})]$, $i\in\bar{\mathcal{N}}$, $\bar{u}_{\theta n} = u_{n_F} - \frac{\tan e_{\theta n}}{\eta_{\theta n}}\frac{\partial e_{\theta n}}{\partial\eta_{\theta n}}H_{1n}\frac{\bar{\omega}}{\sin\beta_n}$, $\hat{u}_{\theta i} = -\eta_{\theta i}\frac{\partial\eta_{\theta i}}{\partial e_{\theta i}}(L_{1vi}^2+L_{2vi}^2+L_{1i}^2+L_{2i}^2+L_{\alpha_{i,i_+}}^2)$, $i\in\bar{\mathcal{N}}$, $\hat{u}_{\theta n} = -\eta_{\theta n}\frac{\partial\eta_{\theta n}}{\partial\theta_{\theta n}}(L_{1vn}^2+L_{2vn}^2+L_{1n}^2+L_{2n}^2)$, and $u_{i_F} = \frac{u_{idx}F_y-u_{idy}F_x}{u_{i_Tu_{id}}^2}$ with $L_{1vi} = L_{1i}\cos(\phi_i-\theta_i)v_i$, $L_{2vi} = L_{2i}\sin(\phi_i-\theta_i)v_i$, $L_{1i} = L_{\beta_i}\frac{\sin^2\beta_i}{\cos\beta_i}$, $L_{2i} = L_{\phi_i}\sin\beta_i + L_{\alpha_{i,i_+}}\sin\beta_i$, $i\in\bar{\mathcal{N}}$, $L_{2n} = L_{\phi_n}\sin\beta_n$, $L_{j} = \frac{1}{u_{id}^Tu_{id}}(u_{idx}\frac{\partial u_{idy}}{\partial j}-u_{idy}\frac{\partial u_{idx}}{\partial j})$, $j=\beta_i$, ϕ_i , α_{i,i_+} . Note that the term $\frac{\tan e_{\theta i}}{\eta_{\theta i}}\frac{\partial e_{\theta i}}{\partial\eta_{\theta i}}$ in $\bar{u}_{\theta i}$ will not tend to infinity when the angle error $e_{\theta i}$ in the denominator tends to zero due to the property $\lim_{x\to 0}\frac{\sin x}{x}=1$.

Theorem 1: Under Assumptions 1–2, consider robot kinematics (1) and the dynamics (2) with the control laws (18) and (19), and the adaptive laws (20) and (21), then we have the following results.

- (i) Every robot can avoid collisions with the target and its next-neighbouring robot, while guaranteeing the limited sensing requirement during the encircling motion.
- (ii) The subtended angle $\beta_i(t)$ and the separation angle $\alpha_{i,i_+}(t)$ eventually converge to a small neighborhood of the desired angles $\beta_{\mathrm{des},i}$ and $\alpha_{\mathrm{des},i,i_+}$, respectively.
- (iii) The estimation error $\tilde{v}_{i0}(t)$, the dynamics of bearing angle $\phi_i(t)$, and the signal $u_i(t)$ are bounded.

Proof: (i) Consider the Lyapunov function for the robot n as

$$V_n = \frac{r_0}{2} \eta_{\beta n}^2 + \frac{1}{2\gamma_n} \tilde{v}_{n0}^2 \tag{24}$$

whose derivative along (2), (6), (8), (17), the control law (19), and the adaptive law (21) produces

$$\dot{V}_{n} = -k_{1n}\bar{\Omega}_{\beta n}\underline{\Omega}_{\beta n}\frac{\partial\eta_{\beta n}}{\partial e_{\beta n}}\eta_{\beta n}^{2} - \sigma_{n}\tilde{v}_{n0}^{2} - \sigma_{n}\tilde{v}_{n0}\bar{v}_{0}$$

$$+ r_{0}\eta_{\beta n}\frac{\partial\eta_{\beta n}}{\partial\bar{\Omega}_{\beta n}}\dot{\Omega}_{\beta n} - \left(\eta_{\beta n}\frac{\partial\eta_{\beta n}}{\partial\bar{\Omega}_{\beta n}}\dot{\Omega}_{\beta n}\right)^{2}$$

$$+ r_{0}\eta_{\beta n}\frac{\partial\eta_{\beta n}}{\partial\underline{\Omega}_{\beta n}}\dot{\underline{\Omega}}_{\beta n} - \left(\eta_{\beta n}\frac{\partial\eta_{\beta n}}{\partial\underline{\Omega}_{\beta n}}\dot{\underline{\Omega}}_{\beta n}\right)^{2}$$

$$- H_{1n}\varphi_{n}^{T}v_{0} - \bar{v}_{0}\frac{H_{1n}^{2}}{\sqrt{H_{1n}^{2} + \varepsilon^{2}}}.$$
(25)

By completion of squares, we have

$$r_0 \eta_j \frac{\partial \eta_j}{\partial \bar{\Omega}_j} \dot{\bar{\Omega}}_j \le \frac{1}{2} \left(\eta_j \frac{\partial \eta_j}{\partial \bar{\Omega}_j} \dot{\bar{\Omega}}_j \right)^2 + \frac{r_0^2}{2}, \ j = \beta i, \alpha i$$
 (26)

$$r_0 \eta_j \frac{\partial \eta_j}{\partial \underline{\Omega}_i} \dot{\underline{\Omega}}_j \leq \frac{1}{2} \left(\eta_j \frac{\partial \eta_j}{\partial \underline{\Omega}_j} \dot{\underline{\Omega}}_j \right)^2 + \frac{r_0^2}{2}, \ j = \beta i, \alpha i$$
 (27)

$$-\sigma_i \tilde{\tilde{v}}_{i0} \bar{v}_0 \le \frac{\sigma_i}{2} \tilde{\tilde{v}}_{i0}^2 + \frac{\sigma_i}{2} \bar{v}_0^2, \ i \in \mathcal{N}.$$
 (28)

For the term $\bar{\Omega}_{\beta n} \underline{\Omega}_{\beta n} \frac{\partial \eta_{\beta n}}{\partial e_{\beta n}}$ in (25), it follows from (17) that

$$\bar{\Omega}_{j}\underline{\Omega}_{j}\frac{\partial \eta_{j}}{\partial e_{j}} = \frac{(\bar{\Omega}_{j}\underline{\Omega}_{j})^{2}(\bar{\Omega}_{j}\underline{\Omega}_{j} + e_{j}^{2})}{(\bar{\Omega}_{j} - e_{j})^{2}(e_{j} + \underline{\Omega}_{j})^{2}} > \eta_{j}^{2}, \ j = \beta i, \alpha i.$$
 (29)

Moreover, in (25), we have $-H_{1i}\varphi_i^Tv_0 \leq ||H_{1i}\varphi_i^T|| ||v_0|| \leq |H_{1i}|\bar{v}_0$, and thus in view of Lemma 1, the following inequality

$$|H_{1i}|\bar{v}_0 - \bar{v}_0 \frac{H_{1i}^2}{\sqrt{H_{1i}^2 + \varepsilon^2}} < \varepsilon \bar{v}_0, \ i \in \mathcal{N}$$
 (30)

holds. Substituting (26)–(30) into (25) yields

$$\dot{V}_n < -k_{1n}\eta_{\beta n}^4 - \frac{\sigma_n}{2}\tilde{v}_{n0}^2 + \frac{\sigma_n}{2}\bar{v}_0^2 + \varepsilon\bar{v}_0 + r_0^2. \tag{31}$$

Completing the squares, for any variable $x \in \mathbb{R}$, we obtain

$$(x^2 - 1)^2 > 0 \Rightarrow -x^4 < -2x^2 + 1.$$
 (32)

Hence, it follows from (24) that \dot{V}_n in (31) leads to $\dot{V}_n < -\mu_n V_n + C_n$, where $\mu_n = \min\{\frac{4k_{1n}^{\frac{1}{2}}}{r_0}, \sigma_n \gamma_n\}$ and $C_n = \frac{\sigma_n}{2}\bar{v}_0^2 + \varepsilon\bar{v}_0 + r_0^2 + 1$, which implies that

$$V_n < (V_{n0} - \frac{C_n}{\mu_n}) \exp(-\mu_n t) + \frac{C_n}{\mu_n}.$$
 (33)

It follows from (24) and (33) that $\eta_{\beta n}$ and \tilde{v}_{n0} are bounded. Hence, the precision constraint (14) is never violated according to (16), which further satisfies the constraint requirement (9).

As a result, the constraint imposed on the subtended angle (7) is guaranteed, which implies that, in view of (5), the relative distance $\rho_n(t)$ is also bounded, i.e., $0<\underline{\rho}_n<\rho_n(t)<\bar{\rho}_n$.

Consider the Lyapunov function for the robot $i, i \in \overline{\mathcal{N}}$, as

$$V_i = \frac{r_0}{2} \eta_{\beta i}^2 + \frac{r_0}{2} \eta_{\alpha i}^2 + \frac{1}{2\gamma_i} \tilde{v}_{i0}^2$$
 (34)

whose derivative along (2), (6), (8), (12), (17), (22), (23), the control law (18), and the adaptive law (20) gives

$$\dot{V}_{i} = -k_{1i}\bar{\Omega}_{\beta i}\underline{\Omega}_{\beta i}\frac{\partial\eta_{\beta i}}{\partial e_{\beta i}}\eta_{\beta i}^{2} - k_{2i}\bar{\Omega}_{\alpha i}\underline{\Omega}_{\alpha i}\frac{\partial\eta_{\alpha i}}{\partial e_{\alpha i}}\eta_{\alpha i}^{2}
+ r_{0}\eta_{\beta i}\frac{\partial\eta_{\beta i}}{\partial\bar{\Omega}_{\beta i}}\dot{\bar{\Omega}}_{\beta i} - \left(\eta_{\beta i}\frac{\partial\eta_{\beta i}}{\partial\bar{\Omega}_{\beta i}}\dot{\bar{\Omega}}_{\beta i}\right)^{2} - H_{1i}\varphi_{i}^{T}v_{0}
+ r_{0}\eta_{\beta i}\frac{\partial\eta_{\beta i}}{\partial\underline{\Omega}_{\beta i}}\dot{\underline{\Omega}}_{\beta i} - \left(\eta_{\beta i}\frac{\partial\eta_{\beta i}}{\partial\underline{\Omega}_{\beta i}}\dot{\underline{\Omega}}_{\beta i}\right)^{2} - H_{2i}\bar{\varphi}_{i}^{T}v_{0}
+ r_{0}\eta_{\alpha i}\frac{\partial\eta_{\alpha i}}{\partial\bar{\Omega}_{\alpha i}}\dot{\bar{\Omega}}_{\alpha i} - \left(\eta_{\alpha i}\frac{\partial\eta_{\alpha i}}{\partial\bar{\Omega}_{\alpha i}}\dot{\bar{\Omega}}_{\alpha i}\right)^{2} - \bar{v}_{0}\frac{H_{1i}^{2}}{\sqrt{H_{1i}^{2} + \varepsilon^{2}}}
+ r_{0}\eta_{\alpha i}\frac{\partial\eta_{\alpha i}}{\partial\underline{\Omega}_{\alpha i}}\dot{\underline{\Omega}}_{\alpha i} - \left(\eta_{\alpha i}\frac{\partial\eta_{\alpha i}}{\partial\underline{\Omega}_{\alpha i}}\dot{\underline{\Omega}}_{\alpha i}\right)^{2} - \bar{v}_{0}\frac{H_{2i}^{2}}{\sqrt{H_{2i}^{2} + \varepsilon^{2}}}
- r_{0}\eta_{\alpha i}\frac{\partial\eta_{\alpha i}}{\partial e_{\alpha i}}\dot{\phi}_{i+} - \left(\eta_{\alpha i}\frac{\partial\eta_{\alpha i}}{\partial e_{\alpha i}}\right)^{2} - \sigma_{i}\tilde{v}_{i0}\hat{v}_{i0}. \tag{35}$$

By completion of squares, we have

$$-r_0 \eta_{\alpha i} \frac{\partial \eta_{\alpha i}}{\partial e_{\alpha i}} \dot{\phi}_{i_+} \le \frac{1}{2} \left(\eta_{\alpha i} \frac{\partial \eta_{\alpha i}}{\partial e_{\alpha i}} \right)^2 + \frac{1}{2} \left(r_0 \dot{\phi}_{i_+} \right)^2. \tag{36}$$

Substituting (26)–(30), (32), and (36) into (35) yields

$$\dot{V}_{i} < -2k_{1i}^{\frac{1}{2}}\eta_{\beta i}^{2} - 2k_{2i}^{\frac{1}{2}}\eta_{\alpha i}^{2} - \frac{\sigma_{i}}{2}\tilde{v}_{i0}^{2} + \frac{1}{2}\left(r_{0}\dot{\phi}_{i_{+}}\right)^{2} + C_{i}^{*}$$
(37)

with $C_i^* = 2\varepsilon \bar{v}_0 + 2r_0^2 + \frac{\sigma_i}{2}\bar{v}_0^2 + 2$, which implies that the convergence of V_i requires the boundedness of $\dot{\phi}_{i_+}$, i.e., $|\dot{\phi}_{i_+}| \leq C_{\phi i_+}$. In view of (2), (5), (23), and the control law (19), the bearing angle dynamics for the robot n is given by

$$\dot{\phi}_n = \frac{\bar{\omega}}{r_0} - \frac{\bar{\varphi}_n^T v_0}{\rho_n} \tag{38}$$

where $\bar{\omega}>0$ is a design parameter, r_0 is the disk target's radius, $\bar{\varphi}_n^T$ is the unit vector, v_0 is the target's velocity with $||v_0||\leq \bar{v}_0$, and $0<\rho_n<\rho_n$ according to (33). Hence, the dynamics $\dot{\phi}_n$ is bounded, i.e., $|\dot{\phi}_n|\leq C_{\phi n}$, which implies that $\dot{V}_i<-\mu_iV_i+C_i$ holds for i=n-1, in view of (34) and (37), where $\mu_i=\min\{\frac{4k_{1i}^{\frac{1}{2}}}{r_0},\frac{4k_{2i}^{\frac{1}{2}}}{r_0},\sigma_i\gamma_i\}$ and $C_i=C_i^*+\frac{1}{2}(r_0C_{\phi i_+})^2$, with $C_{\phi i_+}=C_{\phi n}$. Then, we have

$$V_i < (V_{i0} - \frac{C_i}{\mu_i}) \exp(-\mu_i t) + \frac{C_i}{\mu_i}.$$
 (39)

It follows from (34) and (39) that $\eta_{\beta i}$, $\eta_{\alpha i}$, and \tilde{v}_{i0} are bounded. Hence, the precision constraints (14) and (15) are never violated according to (16), which further satisfies the constraint requirements (9) and (13). As a result, the constraints imposed on the subtended angle (7) and the separation angle (11) are guaranteed, which implies that, in view of (5), the relative distance $\rho_i(t)$ is also bounded, i.e., $0 < \rho_i < \rho_i(t) < \bar{\rho}_i$.

According to (2), (23), and the control law (18), the bearing angle dynamics for the robot i is given by

$$\dot{\phi}_i = \frac{1}{\rho_i} \left(u_{2i} - \hat{\bar{v}}_{i0} \frac{H_{2i}}{\sqrt{H_{2i}^2 + \varepsilon^2}} \right) - \frac{\bar{\varphi}_i^T v_0}{\rho_i} \tag{40}$$

where ρ_i , $e_{\alpha i}$, and $\hat{\overline{v}}_{i0}$ are bounded due to the boundedness of $\eta_{\beta i}$, $\eta_{\alpha i}$, and $\tilde{\overline{v}}_{i0}$. Furthermore, it is clear that $\frac{\partial e_{\alpha i}}{\partial \Omega_{\alpha i}}$, $\frac{\partial e_{\alpha i}}{\partial \Omega_{\alpha i}}$, $\frac{\partial e_{\alpha i}}{\partial \Omega_{\alpha i}}$, and $\frac{\partial e_{\alpha i}}{\partial e_{\alpha i}}$ are bounded, since the constraint (15) is guaranteed. As a result, the dynamics $\dot{\phi}_i$ for the robot i-1 is bounded, which implies that \dot{V}_i in (37) for the robot i, $i \in \bar{\mathcal{N}}$, can yield (39). It is concluded from (33) and (39) that $\eta_{\beta i}$, $i \in \mathcal{N}$, and $\eta_{\alpha i}$, $i \in \bar{\mathcal{N}}$, are bounded. Therefore, the constraints on the subtended angle β_i in (7) and the separation angle α_{i,i_+} in (11) are never violated, which means that the limited sensing requirement and collision avoidance with the moving target and the next-neighbouring robot are guaranteed.

(ii) In terms of (33) and (39), we have $V_i < \frac{C_i}{\mu_i}$ as $t \to \infty$, which implies that $\eta_{\beta i}$ and $\eta_{\alpha i}$ will converge into the sets $\{\eta_{\beta i}: |\eta_{\beta i}| < \sqrt{\frac{2C_i}{r_0\mu_i}}, i \in \mathcal{N}\}$ and $\{\eta_{\alpha i}: |\eta_{\alpha i}| < \sqrt{\frac{2C_i}{r_0\mu_i}}, i \in \bar{\mathcal{N}}\}$, respectively. The size of convergence is directly associated with $k_{1i}, k_{2i}, \sigma_i, \gamma_i, \varepsilon, C_{\phi i_+}, \bar{v}_0$, and r_0 . Furthermore, from (16), we have that as $t \to \infty$, the errors $e_{\beta i}$ and $e_{\alpha i}$ will converge into the sets $\{e_j: -\underline{\Lambda}_j \leq e_j \leq \bar{\Lambda}_j\}$, where $\underline{\Lambda}_j = \frac{\varrho \Omega_j - \varrho \bar{\Omega}_j - \bar{\Omega}_j \Omega_j}{2\varrho} + \frac{\sqrt{(\varrho \Omega_j - \varrho \bar{\Omega}_j - \bar{\Omega}_j \Omega_j)^2 + 4\varrho^2 \bar{\Omega}_j \Omega_j}}{2\varrho}$, with $\varrho = \sqrt{\frac{2C_i}{r_0\mu_i}}, \ j = \beta i, \alpha i$. Using the L' Hopital's rule, we obtain $\lim_{\varrho \to 0} \underline{\Lambda}_j = 0$ and $\lim_{\varrho \to 0} \bar{\Lambda}_j = 0$, which indicates that a small C_i and a large μ_i are preferred such that the errors $e_{\beta i}$ and $e_{\alpha i}$ will converge to small neighbourhoods of the origin. For a large μ_i , large design parameters k_{1i}, k_{2i} , and γ_i are desirable. To obtain a small C_i , a small tuning number ε is favored. As a result, the subtended angle β_i and the separation angle α_{i,i_+} eventually converge to a small neighborhood of the desired angles $\beta_{\text{des},i}$ and $\alpha_{\text{des},i,i_+}$, respectively.

(iii) Now, we recall from (33) and (39) that $\frac{1}{2\gamma_i}\tilde{v}_{i0}^2 < (V_{i0} - \frac{C_i}{\mu_i}) \exp(-\mu_i t) + \frac{C_i}{\mu_i} \leq c_0$, where c_0 is the upper bound of initial condition, which implies $|\bar{v}_{i0}| < \sqrt{2\gamma_i c_0}$. Furthermore, $\lim_{t\to\infty} V_i < \frac{C_i}{\mu_i}$ implies that the estimation error \tilde{v}_{i0} is ultimately uniformly bounded by $\sqrt{\frac{2\gamma_i C_i}{\mu_i}}$. In view of (38) and (40), the dynamics of bearing angle $\dot{\phi}_i$ is bounded. The signal u_i is also bounded due to the boundedness of η_j , e_j , $\bar{\Omega}_j$, $\underline{\Omega}_j$, $\dot{\Omega}_j$, $\dot{\Omega}_j$, $\dot{\Omega}_j$, j, j = αi , βi , and \hat{v}_{i0} .

Remark 7: Based on the bearing-only measurement, the presented angle constrained strategy limits to the disk target. Regarding to cases where the target is not circular, the proposed constrained control framework is also compatible for the position measurement. The orthogonal-vector-based control design incorporated with universal BLFs has advantages in constrained target enclosing problem, in which the formation errors to be constrained can be distance or angle errors along two orthogonal directions. In addition, universal BLFs can handle the constraints with different types (asymmetric or symmetric) and nature (time-varying or time-invariant) in a

uniform framework. Specifically, the enclosing formation is partially specified by the relative distance $\rho_i(t)$ in (4), instead of the subtended angle. Consequently, the distance error $e_{\rho i}(t) = \rho_i(t) - r_{\mathrm{des},i}$ is imposed on both safety and precision constraints, that is, $-\underline{e}_{\rho i} \leq -\underline{\Omega}_{\rho i}(t) < e_{\rho i}(t) < \bar{\Omega}_{\rho i}(t) \leq \bar{e}_{\rho i}$ where $\underline{e}_{\rho i} = r_{\mathrm{des},i} - \underline{\rho}_i$ and $\bar{e}_{\rho i} = \bar{\rho}_i - r_{\mathrm{des},i}$ with $r_{\mathrm{des},i}$ being the desired radius, and $\underline{\rho}_i$ and $\bar{\rho}_i$ respectively being the lower and upper bounds of $\rho_i(t)$. Then, the position-based controllers are designed as $u_i = G_i^{-1}(\varphi_i u_{1i} + \bar{\varphi}_i u_{2i}\rho_i - \varphi_i \hat{u}_{1i} - \bar{\varphi}_i \hat{u}_{2i})$, $i \in \bar{\mathcal{N}}$, and $u_i = G_i^{-1}(\varphi_i u_{1i} - \varphi_i \hat{u}_{1i} + \bar{\varphi}_i \bar{\omega}_{\rho i})$, i = n, where $u_{1i} = -k_{1i}\bar{\Omega}_{\rho i}\underline{\Omega}_{\rho i}\eta_{\rho i} - \frac{\partial e_{\rho i}}{\partial \Omega_{\rho i}}\bar{\Omega}_{\rho i} - \frac{\partial e_{\rho i}}{\partial \Omega_{\rho i}}\bar{\Omega}_{\rho i}$, $u_{2i} = -k_{2i}\bar{\Omega}_{\alpha i}\underline{\Omega}_{\alpha i}\eta_{\alpha i} - \frac{\partial e_{\alpha i}}{\partial \Omega_{\alpha i}}\bar{\Omega}_{\alpha i} - \frac{\partial e_{\alpha i}}{\partial \Omega_{\alpha i}}\bar{\Omega}_{\alpha i} - \eta_{\alpha i}\frac{\partial \eta_{\alpha i}}{\partial e_{\alpha i}}$, $u_{1i} = \eta_{\rho i}\frac{\partial \eta_{\rho i}}{\partial e_{\rho i}}$, and $u_{2i} = -\frac{\partial \alpha_{i}}{\partial \Omega_{\alpha i}}\bar{\Omega}_{\alpha i}$ with φ_i being the unit vector from the target pointing to the onboard sensor.

Remark 8: When the precision constraints (14) and (15) are not considered, the transformed error given in (16) becomes $\eta_j = \frac{\bar{e}_j \underline{e}_j e_j}{(\bar{e}_j - e_j)(e_j + \underline{e}_j)}$ where the constraints are time-invariant in view of (9) and (13). Accordingly, in control laws (18) and (19), terms u_{1i} and u_{2i} become $u_{1i} = \frac{\cos \beta_i}{\sin^2 \beta_i} (-k_{1i} \bar{e}_{\beta i} \underline{e}_{\beta i} \eta_{\beta i})$ and $u_{2i} = \frac{1}{\sin \beta_i} (-k_{2i} \bar{e}_{\alpha i} \underline{e}_{\alpha i} \eta_{\alpha i} - \eta_{\alpha i} \frac{\partial \eta_{\alpha i}}{\partial e_{\alpha i}})$, respectively.

IV. SIMULATION STUDIES

A. MATLAB Simulation

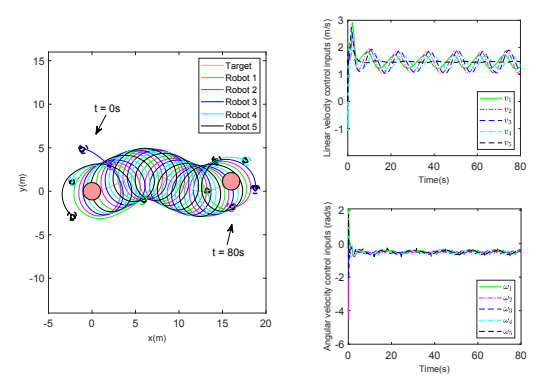
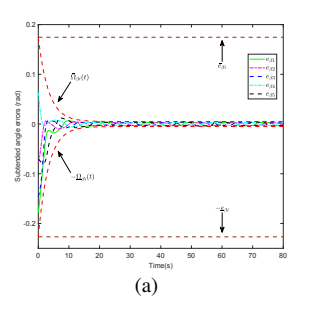


Fig. 2. The phase-plane trajectories with control inputs.

Comparative simulations with and without precision constraints are carried out using the proposed control algorithm, where the mobile robots are expected to surround a target with even distribution. The target moves from $p_0(0) = [0 \ 0]^T$ with $v_0 = [0.2 \ 0.1 \sin(0.1t)]^T$ m/s which is unknown to all robots. The onboard sensor is shifted a distance d = 0.2m, and the safety radii of the robots and the target are $r_i = 0.5$ m and $r_0 = 1$ m, respectively. The angle constraints are selected as $\beta_{\min,i} = 7\pi/180$ rad, $\beta_{\max,i} = \pi/6$ rad, $\underline{\alpha}_{i,i_+} = \pi/6$ rad, and $\bar{\alpha}_{i,i_+}=11\pi/24$ rad such that $\underline{\alpha}_{5,1}=2\pi-\sum \bar{\alpha}_{i,i_+}=\pi/6$ rad. The desired angles are set as $\beta_{\text{des},i} = \pi/9\text{rad}$, $i \in \mathcal{N}$, and $\alpha_{{
m des},i,i_+}=2\pi/5{
m rad},\,i\in\bar{\mathcal{N}}.$ The precision constraint functions are taken as $\underline{\Omega}_{\beta i}(t) = (\underline{e}_{\beta i} - 0.005) \exp(-0.3t) + 0.005$, $\bar{\Omega}_{\beta i}(t) = (\bar{e}_{\beta i} - 0.005) \exp(-0.3t) + 0.005, \ \underline{\Omega}_{\alpha i}(t) =$ $(\underline{e}_{\alpha i} - 0.012) \exp(-0.3t) + 0.012$, and $\bar{\Omega}_{\alpha i}(t) = (\bar{e}_{\alpha i} - 0.012) \exp(-0.3t)$ $0.012) \exp(-0.3t) + 0.012$, where $\underline{e}_{\beta i} = 13\pi/180$, $\bar{e}_{\beta i} =$ $\pi/18$, $\underline{e}_{\alpha i}=7\pi/30$, and $\bar{e}_{\alpha i}=7\pi/120$ according to (9) and (13). The design parameters are $k_{1i}=2$, $k_{2i}=5$, $\gamma_i=15$, $i \in \mathcal{N}$, $\sigma_1 = 0.1$, $\sigma_i = 0.01$, $i \in \mathcal{N} \setminus 1$, $\varepsilon = 0.01$, and $\bar{\omega} = 0.5$.



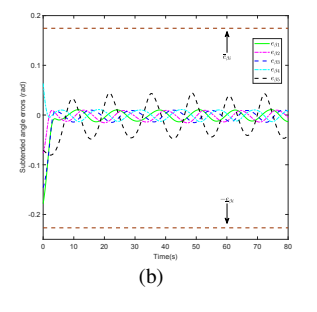
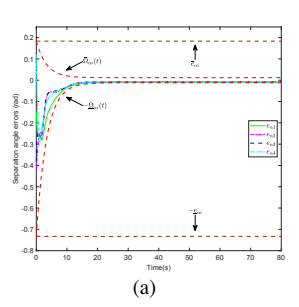


Fig. 3. The profiles of subtended angle errors. (a) The proposed controller. (b) The controller without precision constraints.



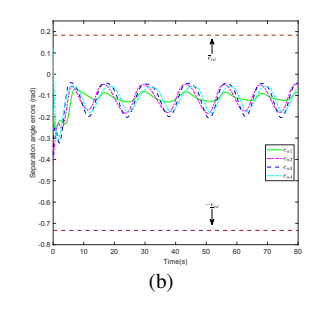


Fig. 4. The profiles of separation angle errors. (a) The proposed controller. (b) The controller without precision constraints.

The initial states of the robots are $[x_1 \ y_1 \ \theta_1]^T = [6 \ -1 \ -\pi]^T, [x_2 \ y_2 \ \theta_2]^T = [2 \ 3 \ 0]^T, [x_3 \ y_3 \ \theta_3]^T = [-1.2 \ 4.8 \ \pi/12]^T, [x_4 \ y_4 \ \theta_4]^T = [-2.3 \ 1 \ \pi/3]^T, [x_5 \ y_5 \ \theta_5]^T = [-2.2 \ -3 \ 2\pi/3]^T,$ and $\hat{v}_{i0} = 0, \ i \in \mathcal{N}.$ The design parameters in the comparative simulations are the same except for $\sigma_1 = 0.01.$

The trajectories of the target and robots with the control inputs are plotted in Fig. 2, where the moving target is tracked and enclosed by n=5 mobile robots. As shown in Figs. 3–4, the subtended angle errors and the separation angle errors with and without precision constraints always evolve within safety constraints, which implies that the limited sensing requirement and collision avoidance with the target and neighbouring robots are guaranteed. However, without the consideration of precision constraints (see the controllers discussed in Remark 8), the subtended and separation angle errors deviate farther from the origin (see Figs. 3(b)–4(b)). In contrast, without the knowledge of target's velocity v_0 and the dynamics of bearing angle $\dot{\phi}_{i_+}$, the control laws (18) and (19) ensure the precision constraint requirements such that all angle errors converge to small neighbourhoods of zero.

B. Gazebo Simulation

An uneven distribution of the robots surrounding a target is further conducted using Gazebo simulator on ROS. The same robot model is used to emulate a disk target with the radius of $r_0=1$ m. The target is assigned to track the trajectory $[x_t \ y_t]^T=[-10\sin(-0.02t)\ 10\cos(-0.02t)\ -10]^T$ from the initial pose of $[x_0 \ y_0 \ \theta_0]^T=[0\ 0\ 0]^T$. The angle constraints are selected as $\beta_{\min,i}=7\pi/180\text{rad}$, $\beta_{\max,i}=\pi/6\text{rad}$, $\underline{\alpha}_{i,i+}=\pi/6\text{rad}$, $\bar{\alpha}_{1,2}=66\pi/180\text{rad}$, and $\bar{\alpha}_{i,i+}=88\pi/180\text{rad}$, i=2,3,4. The onboard sensor is shifted a distance d=0.2m. The desired angles are set

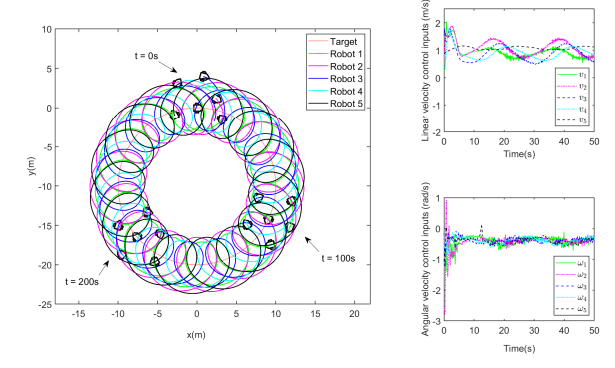


Fig. 5. The phase-plane trajectories with control inputs in the Gazebo simulation

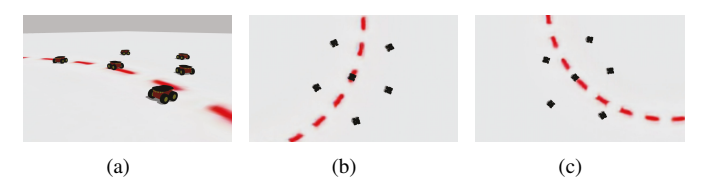
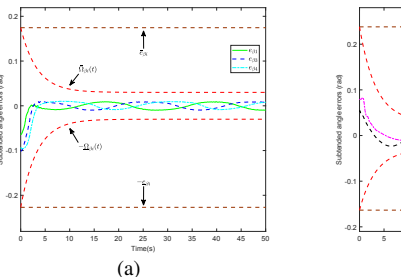


Fig. 6. Snapshots taken in Gazebo. (a) t = 0s. (b) t = 100s. (c) t = 200s.

as $\beta_{\mathrm{des},i} = \pi/9\mathrm{rad},\ i = 1,3,4,\ \beta_{\mathrm{des},i} = \pi/11\mathrm{rad},\ i = 2,5,\ \alpha_{\mathrm{des},1,2} = \pi/3\mathrm{rad},\ \mathrm{and}\ \alpha_{\mathrm{des},i,i_+} = 4\pi/9\mathrm{rad},\ i = 2,3,4.$ The precision constraint functions are designed as $\underline{\Omega}_{\beta i}(t) = (\underline{e}_{\beta i} - 0.03)\exp(-0.3t) + 0.03,\ \overline{\Omega}_{\beta i}(t) = (\bar{e}_{\beta i} - 0.03)\exp(-0.3t) + 0.03,\ \underline{\Omega}_{\alpha i}(t) = (\underline{e}_{\alpha i} - 0.05)\exp(-0.3t) + 0.05,\ \mathrm{and}\ \overline{\Omega}_{\alpha i}(t) = (\bar{e}_{\alpha i} - 0.05)\exp(-0.3t) + 0.05.$ The design parameters are selected as $k_{1i} = 0.5,\ k_{2i} = 5,\ \gamma_i = 0.01,\ \sigma_i = 0.01,\ \varepsilon = 0.008,\ \mathrm{and}\ \overline{\omega} = 0.3.$ The initial states of the robots are $[x_1\ y_1\ \theta_1]^T = [3.2\ -1.4\ -5\pi/9]^T,\ [x_2\ y_2\ \theta_2]^T = [2.4\ 1.2\ -\pi/6]^T,\ [x_3\ y_3\ \theta_3]^T = [0.8\ 4\ -\pi/12]^T,\ [x_4\ y_4\ \theta_4]^T = [-2.5\ 3\ \pi/3]^T,\ [x_5\ y_5\ \theta_5]^T = [-2.8\ -1\ 2\pi/3]^T,\ \mathrm{and}\ \hat{v}_{i0} = 0,\ i\in\mathcal{N}.$

The trajectories, control inputs, and different snapshot moments are demonstrated in Figs 5-6. Both subtended and



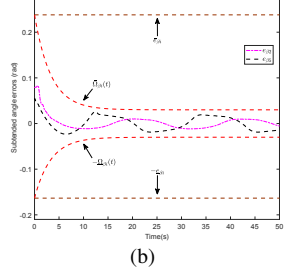
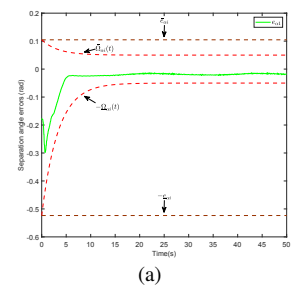


Fig. 7. The profiles of subtended angle errors in the Gazebo simulation.



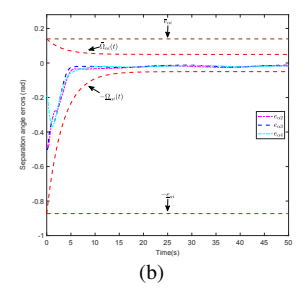


Fig. 8. The profiles of separation angle errors in the Gazebo simulation.

separation angle errors stay within their corresponding constraints, and converge to small neighbourhoods of zero shown in Figs. 7–8, which implies the safety and precision constraint requirements are satisfied.

V. CONCLUSION

This paper proposes a constrained control framework to solve the moving-target enclosing problem for nonholonomic multirobot systems with safety and precision constraints. The target-robot and inter-robot angles obtained from bearing measurements are constrained to satisfy the requirements of limited sensing range and collision avoidance. The precision constraint further guarantees all robots converging to a small neighbourhood of the desired enclosing formation. Universal BLFs and adaptive estimators are incorporated with control design to handle different constraint requirements, despite the lack of target's velocity.

REFERENCES

- [1] K.-K. Oh, M.-C. Park, and H.-S. Ahn, "A survey of multi-agent formation control," *Automatica*, vol. 53, no. 3, pp. 424–440, 2015.
- [2] X. Yu, L. Liu, and G. Feng, "Distributed circular formation control of nonholonomic vehicles without direct distance measurements," *IEEE Transactions on Automatic Control*, vol. 63, no. 8, pp. 2730–2737, 2018.
- [3] R. S. Sharma, A. Mondal, and L. Behera, "Tracking control of mobile robots in formation in the presence of disturbances," *IEEE Transactions* on *Industrial Informatics*, vol. 17, no. 1, pp. 110–123, 2021.
- [4] M. Lv, B. De Schutter, and S. Baldi, "Nonrecursive control for formation-containment of HFV swarms with dynamic event-triggered communication," *IEEE Transactions on Industrial Informatics*, vol. 19, no. 3, pp. 3188–3197, 2023.
- [5] H. Yamaguchi, "A cooperative hunting behavior by mobile-robot troops," The International Journal of Robotics Research, vol. 18, no. 9, pp. 931–940, 1999.
- [6] Y. Lan, G. Yan, and Z. Lin, "Distributed control of cooperative target enclosing based on reachability and invariance analysis," *Systems & Control Letters*, vol. 59, no. 7, pp. 381–389, 2010.
- [7] I. Shames, S. Dasgupta, B. Fidan, and B. D. O. Anderson, "Circumnavigation using distance measurements under slow drift," *IEEE Transactions on Automatic Control*, vol. 57, no. 4, pp. 889–903, 2012.
- [8] R. Li, Y. Shi, and Y. Song, "Localization and circumnavigation of multiple agents along an unknown target based on bearing-only measurement: A three dimensional solution," *Automatica*, vol. 94, pp. 18–25, 2018.
- [9] G. López-Nicolás, M. Aranda, and Y. Mezouar, "Adaptive multirobot formation planning to enclose and track a target with motion and visibility constraints," *IEEE Transactions on Robotics*, vol. 36, no. 1, pp. 142–156, 2020.
- [10] L. Dou, C. Song, X. Wang, L. Liu, and G. Feng, "Target localization and enclosing control for networked mobile agents with bearing measurements," *Automatica*, vol. 118, 2020.
- [11] R. Zheng, Y. Liu, and D. Sun, "Enclosing a target by nonholonomic mobile robots with bearing-only measurements," *Automatica*, vol. 53, pp. 400–407, 2015.
- [12] Z. Yang, C. Chen, S. Zhu, X. Guan, and G. Feng, "Distributed entrapping control of multiagent systems using bearing measurements," *IEEE Transactions on Automatic Control*, vol. 66, no. 12, pp. 5696–5710, 2021.
- [13] T.-H. Kim and T. Sugie, "Cooperative control for target-capturing task based on a cyclic pursuit strategy," *Automatica*, vol. 43, no. 8, pp. 1426– 1431, 2007.
- [14] M. Deghat, I. Shames, B. D. O. Anderson, and C. Yu, "Localization and circumnavigation of a slowly moving target using bearing measurements," *IEEE Transactions on Automatic Control*, vol. 59, no. 8, pp. 2182–2188, 2014.
- [15] C. Wang and G. Xie, "Limit-cycle-based decoupled design of circle formation control with collision avoidance for anonymous agents in a plane," *IEEE Transactions on Automatic Control*, vol. 62, no. 12, pp. 6560–6567, 2017.

- [16] L. Kou, Z. Chen, and J. Xiang, "Cooperative fencing control of multiple vehicles for a moving target with an unknown velocity," *IEEE Transac*tions on Automatic Control, vol. 67, no. 2, pp. 1008–1015, 2022.
- [17] C. Wang, W. Xia, and G. Xie, "Limit-cycle-based design of formation control for mobile agents," *IEEE Transactions on Automatic Control*, vol. 65, no. 8, pp. 3530–3543, 2020.
- [18] L. Dou, X. Yu, L. Liu, X. Wang, and G. Feng, "Moving-target enclosing control for mobile agents with collision avoidance," *IEEE Transactions* on Control of Network Systems, vol. 8, no. 4, pp. 1669–1679, 2021.
- [19] M. Basiri, A. N. Bishop, and P. Jensfelt, "Distributed control of triangular formations with angle-only constraints," *Systems & Control Letters*, vol. 59, no. 2, pp. 147–154, 2010.
- [20] S. Zhao and D. Zelazo, "Bearing rigidity and almost global bearingonly formation stabilization," *IEEE Transactions on Automatic Control*, vol. 61, no. 5, pp. 1255–1268, 2016.
- [21] S. Zhao, Z. Li, and Z. Ding, "Bearing-only formation tracking control of multiagent systems," *IEEE Transactions on Automatic Control*, vol. 64, no. 11, pp. 4541–4554, 2019.
- [22] S. Mastellone, D. M. Stipanović, C. R. Graunke, K. A. Intlekofer, and M. W. Spong, "Formation control and collision avoidance for multi-agent non-holonomic systems: Theory and experiments," *The International Journal of Robotics Research*, vol. 27, no. 1, pp. 107–126, 2008.
- [23] B. S. Park and S. J. Yoo, "Connectivity-maintaining and collision-avoiding performance function approach for robust leader-follower formation control of multiple uncertain underactuated surface vessels," *Automatica*, vol. 127, 2021, Article 109501.
- [24] S.-L. Dai, K. Lu, and J. Fu, "Adaptive finite-time tracking control of nonholonomic multirobot formation systems with limited field-of-view sensors," *IEEE Transactions on Cybernetics*, vol. 52, no. 10, pp. 10695– 10708, 2022.
- [25] X. Jin, S.-L. Dai, and J. Liang, "Adaptive constrained formation-tracking control for a tractor-trailer mobile robot team with multiple constraints," *IEEE Transactions on Automatic Control*, vol. 68, no. 3, pp. 1700–1707, 2023.
- [26] C. P. Bechlioulis and G. A. Rovithakis, "Robust adaptive control of feedback linearizable MIMO nonlinear systems with prescribed performance," *IEEE Transactions on Automatic Control*, vol. 53, no. 9, pp. 2090–2099, 2008.
- [27] ——, "Decentralized robust synchronization of unknown high order nonlinear multi-agent systems with prescribed transient and steady state performance," *IEEE Transactions on Automatic Control*, vol. 62, no. 1, pp. 123–134, 2017.
- [28] F. Mehdifar, C. P. Bechlioulis, F. Hashemzadeh, and M. Baradarannia, "Prescribed performance distance-based formation control of multi-agent systems," *Automatica*, vol. 119, 2020, Article 109086.
- [29] X. Jin, S.-L. Dai, and J. Liang, "Fixed-time path-following control of an autonomous vehicle with path-dependent performance and feasibility constraints," *IEEE Transactions on Intelligent Vehicles*, vol. 8, no. 1, pp. 458–468, 2023.
- [30] X. Jin, "Fault tolerant finite-time leader-follower formation control for autonomous surface vessels with LOS range and angle constraints," *Automatica*, vol. 68, pp. 228–236, 2016.
- [31] K. Zhao, Y. Song, and Z. Zhang, "Tracking control of MIMO nonlinear systems under full state constraints: A single-parameter adaptation approach free from feasibility conditions," *Automatica*, vol. 107, no. 107, pp. 52–60, 2019.
- [32] K. Lu, S.-L. Dai, and X. Jin, "Fixed-time rigidity-based formation maneuvering for nonholonomic multirobot systems with prescribed performance," *IEEE Transactions on Cybernetics*, Early Access Online, DOI:10.1109/TCYB.2022.3226297, 2022.
- [33] M. Lv, B. De Schutter, C. Shi, and S. Baldi, "Logic-based distributed switching control for agents in power-chained form with multiple unknown control directions," *Automatica*, vol. 137, 2022, Article 110143.
- [34] K. P. Tee, S. S. Ge, and E. H. Tay, "Barrier Lyapunov functions for the control of output-constrained nonlinear systems," *Automatica*, vol. 45, no. 4, pp. 918–927, 2009.
- [35] Y.-J. Liu and S. Tong, "Barrier Lyapunov functions for Nussbaum gain adaptive control of full state constrained nonlinear systems," *Automatica*, vol. 76, pp. 143–152, 2017.
- [36] X. Jin, "Adaptive fixed-time control for MIMO nonlinear systems with asymmetric output constraints using universal barrier functions," *IEEE Transactions on Automatic Control*, vol. 64, no. 7, pp. 3046–3053, 2019.
- [37] C. Wang and Y. Lin, "Decentralized adaptive tracking control for a class of interconnected nonlinear time-varying systems," *Automatica*, vol. 54, pp. 16–24, 2015.